PROCEEDINGS OF SPIE

SPIEDigitalLibrary.org/conference-proceedings-of-spie

EUV reticle print verification with advanced broadband optical wafer inspection and e-Beam review systems

Ravikumar Sanapala, Andrew Cross, Moshe Preil, Jin Qian, Shishir Suman, et al.

Ravikumar Sanapala, Andrew Cross, Moshe Preil, Jin Qian, Shishir Suman, Vidyasagar Anantha, Kaushik Sah, Scott Eitapence, Danilo De Simone, Dieter Van den Heuvel, Philippe Foubert, "EUV reticle print verification with advanced broadband optical wafer inspection and e-Beam review systems," Proc. SPIE 10451, Photomask Technology 2017, 104510L (16 October 2017); doi: 10.1117/12.2281632

SPIE.

Event: SPIE Photomask Technology and EUV Lithography, 2017, Monterey, California, United States

EUV Reticle Print Verification with Advanced Broadband Optical Wafer Inspection and e-Beam Review Systems

Ravikumar Sanapala(1), Andrew Cross(1), Moshe Preil(1), Jin Qian(1), Shishir Suman(1), Vidyasagar Anantha(1), Kaushik Sah(1), Scott Eitapence(1), Danilo De Simone(2), Dieter Van Den Heuvel(2), Philippe Foubert(2)
(1)KLA-Tencor, One Technology Drive, Milpitas, CA 95035
(2)Imec, Kapeldreef 75, 3001 Heverlee, Belgium

ABSTRACT

As the Extreme Ultraviolet (EUV) lithography ecosystem is being actively mapped out to enable sub-7nm design rule devices, there is an immediate and imperative need to identify the EUV reticle (mask) inspection methodologies [1]. The introduction of additional particle sources due to the vacuum system and potential growth of haze defects or other film or particle depositions on the reticle, in combination with pellicle uncertainty pose unique inspection challenges when compared to 193i reticles.

EUV reticles are typically inspected with optical reticle-inspection tools. However, if there is a pellicle on the EUV mask which is non-transmissive to the optical wavelengths used in the reticle inspection tools, then there is a need for alternative inspection methodologies based on inspection of printed wafers. In addition, due to the potential new defect mechanisms associated with the EUV reticles, fabs are looking for additional methods to re-qualify reticles in production using printed wafer inspections. The printed wafer inspection methodology is referred to as “Reticle Print Verification” or “Reticle Print Check.” This paper discusses these alternative inspection methodologies that are being developed in collaboration with imec using an advanced broadband plasma (BBP) patterned wafer optical inspection (KLA-Tencor 3905) and e-beam review systems (KLA-Tencor eDR7280).

Keywords: EUV mask adders, EUV print check, EUV reticle qualification, optical inspection, repeater, EM simulations

1. INTRODUCTION

EUV reticle re-qualification in the wafer fab presents a number of new challenges. Since there will be no actinic inspection tools for at least the next several years, and since the leading pellicle option at the moment does not transmit 193 nm light, we face the possibility of not being able to directly inspect EUV reticles for requal purposes. Optical wafer inspection is an alternative technique for detecting defects on an EUV mask. This technique has certain advantages over mask inspections aside uncertainty on pellicle transmissivity to optical wavelengths. Firstly, we are looking for particles or other depositions on the mask that actually impact printing on wafer. Small size particles or depositions on absorber material may not impact printing on the wafer, while changes in multi-layer reflectivity or phase defects may impact printing but not be visible on the reticle even with e-beam or 193 nm reticle inspection tools. Secondly, with exposure of multiple fields on the wafer (or batch of wafers), we increase the chance of detecting small defects that print on the wafer only as soft repeaters i.e. do not get printed on every field, as opposed to hard repeaters. Thirdly, high throughput of optical inspection coupled with fast e-beam review allows inspection without the need to remove a reticle from the scanner, thereby enabling faster time to results and reducing the potential for adding particles due to additional load/unload cycles in multiple tools.

To conduct this study, a series of programmed defects were designed on a 22nm half-pitch (hp) line-space (L/S) EUV mask. The purpose of these programmed defects is to simulate real defects in order to assess the sensitivity of optical wafer inspection. This mask is then exposed on the EUV scanner (ASML NXE:3300B) on a short-loop wafer. Post development, the wafer is then inspected with KLA-Tencor’s 3905 broadband plasma optical inspection tool to detect and filter the mask defects (location repeaters) that are printed on the wafer. These repeater defects are then imaged in multiple fields by KLA-Tencor’s e-beam review tool to verify the capture rate of printed defects and assess the sensitivity of the optical inspection. Electromagnetic (EM) simulations are also conducted to identify the optimal

Photomask Technology 2017, edited by Peter D. Buck, Emily E. Gallagher, Proc. of SPIE Vol. 10451, 104510L · © 2017 SPIE · CCC code: 0277-786X/17/$18 · doi: 10.1117/12.2281632

stack of the short-loop wafer to further enhance the optical inspection sensitivity to the EUV mask repeaters. These simulations suggested an appropriate underlayer material and thickness that can provide the best optical sensitivity for repeating defects. New EUV resist wafers are then printed with the optimized stack and inspected with the KLA-Tencor 3905 optical inspection tool. The printability of the repeating defects across the wafer is also investigated to assess the size variations. This study has shown that soft repeaters (repeating defects that are not printed on every field) may exist and full-wafer inspection coverage is necessary for the detection of repeaters. An improvement of more than factor of three in terms of defect Signal-to-Noise ratio and up to a factor of nine in capture rate is seen on 3905 inspections with the new optimized stack.

2. EXPERIMENTAL SETUP

Figure 1 shows the mask layout and overview of programmed defects (PD). There are four different flavors of programmed defects namely A, B, C and D types of varying sizes (dimensions are given at wafer level). These programmed defects print as opens/ intrusions for a NTD (negative tone development) process and bridges/ protrusions for a PTD (positive tone development) process. Also, they would get printed as hard or soft repeaters on the wafer depending on their size. It is important to note that very small programmed defects do not print on the wafer at all. PD sizing is known only from design intent and no mask metrology was done to verify them. It was not verified whether they are on the mask as intended in the first place. Hence to have a fair assessment of capture rate from optical wafer inspection, it was important to establish the ground truth on sizing. This was done by a printability study on wafer using KLA-Tencor eBeam review tool, eDR 7280. Also defect sizing was done using the SEM images.

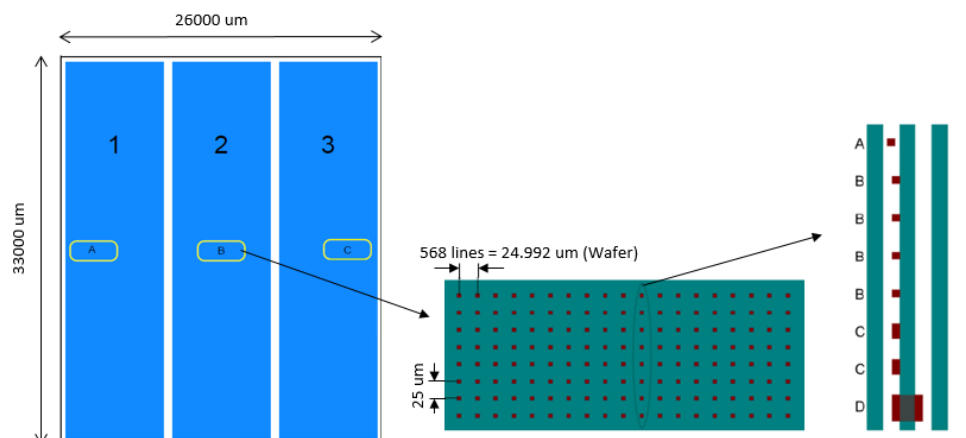

Fig. a

Fig. b

Type	dim	PD1	PD2	PD3	PD4	PD5	PD6	PD7	PD8	PD9	PD10	PD11	PD12	PD13	PD14	PD15	PD16	PD17	PD18	PD19
A	X/Y	4	5	6	7	8	9	10	11	12	13	14	15	16	17	18	19	20	21	22
B	X/Y	4	5	6	7	8	9	10	11	12	13	14	15	16	17	18	19	20	21	22
C	X	4	5	6	7	8	9	10	11	12	13	14	15	16	17	18	19	20	21	22
	Y	8	10	12	14	16	18	20	22	24	26	28	30	32	34	36	38	40	42	44
D	X	26	27	28	29	30	31	32	33	34	35	36	37	38	39	40	41	42	43	44
	Y	13.75	15.75	17.25	19	20.5	21.75	23.25	24.5	26	27.25	28.5	29.75	31	32.25	33.5	34.5	35.75	37	38

Fig. c

Figure 1-a. Design Layout

Figure 1-b. Different types of program defects in the center matrix

Figure 1-c. Intended defect dimensions at wafer level

We used two types of resist materials in our study. Type I is a chemically amplified resist (CAR) with PTD process and Type II is a metal oxide resist with a NTD process. The short loop process of record stacks for both types of resists are shown in Figure 2.

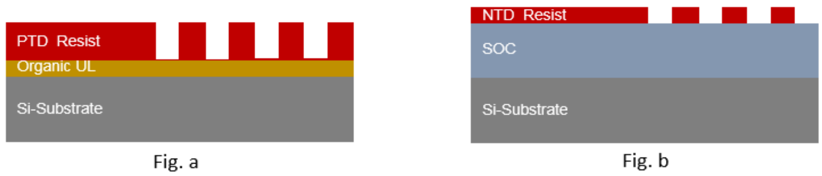

Figure 2-a. POR Stack for CAR PTD Resist

Figure 2-b. POR Stack for metal-oxide NTD Resist

Uniform wafers are exposed and inspected on a 3905 optical inspection tool after development. The optical defect detection recipe is optimized based on capture of these programmed defects. Once a recipe is optimized, multiple field inspection mode is run, and location repeaters identified by the software. These repeaters will include the programmed defects and other *natural* repeaters that are the effect of defects present from mask manufacturing, particles or contamination (?) depositions on the mask. It is the natural repeaters that are important to monitor with time. Any increase can signal mask contamination and trigger control actions.

3. RESULTS AND DISCUSSIONS

3.1 Defect Printability and SEM sizing

Figure 3a shows the result of the printability study on the wafer with metal oxide resist. This was obtained using eDR7280 Critical Point Imaging (CPI) mode, where predefined coordinates within a field can be conveniently imaged across multiple fields. Figure 3b shows SEM sizing analysis (intended vs actual) for PD type B, which print on the wafer as opens or intrusions depending on size.

Decreasing Size ←

15	14	13	12	11	10	9	8	7	6	5	4	3	2	1	PD
0	0	0	0	0	0	100	100	100	100	100	100	100	100	100	A(4)
0	11	11	44	100	100	100	100	100	100	100	100	100	100	100	B(3)
0	11	44	56	100	100	100	100	100	100	100	100	100	100	100	
0	0	0	33	89	100	100	100	100	100	100	100	100	100	100	
0	11	44	89	100	100	100	100	100	100	100	100	100	100	100	
56	100	100	100	100	100	100	100	100	100	100	100	100	100	100	C(2)
33	44	100	100	100	100	100	100	100	100	100	100	100	100	100	
11	44	100	100	89	100	100	100	100	100	100	100	100	100	100	D(1)

(a)

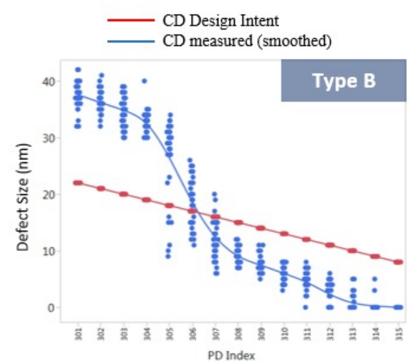

(b)

Figure 3-a. Percentage of locations where a defect was visible on SEM across multiple fields

Figure 3-b. SEM sizing of programmed defects (Type B) compared to design intent

Printability data is used to establish the ground truth against which optical inspection performance is compared. It is worth noting the size variation for the same programmed defect and deviation of the average size from the design intent. The optical defect signal depends on actual defect size and capture rate assessment should be made based on actual defect size rather than intended defect size. (Please note in figure 3-b that actual defect size is lower than intended size from PD 8 onwards).

3.2 Optical Wafer Inspection

Preliminary signal to noise analysis was done using advanced 2935 and 3905 optical inspection systems. Optical signal to noise analysis at programmed defect locations for the wafer with *metal oxide resist* indicated 3905 to have unique programmed defect capture for almost all known repeater locations. Figure 4-a shows the optical signal to noise comparison between 3905 and 2935 for programmed defect of Type B. A full-wafer inspection study was done using 3905. After scanning multiple fields with an optimized recipe, location repeaters were calculated by the software. Figure 4-b shows the detection of programmed defects with optimized sensitivity for the metal oxide resist. The signal to noise ratio is quite low, as indicated in Figure 4-a, and this results in poor detection of PD locations. Figure 4-c further demonstrates capture rate on the full-wafer scan when normalized over average printability data.

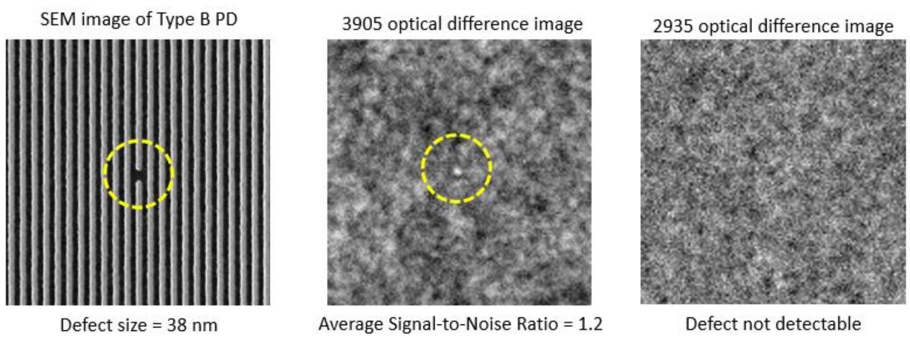

Figure 4-a. Optical signal to noise ratio comparison between 3905 and 2935 for Type B programmed defect on wafer with metal oxide stack

← Decreasing Size

15	14	13	12	11	10	9	8	7	6	5	4	3	2	1	PD
No	No	No	No	No	No	No	No	No	Yes	Yes	Yes	Yes	Yes	Yes	A(4)
No	No	No	No	No	No	No	No	No	No	Yes	Yes	Yes	Yes	Yes	B(3)
No	No	No	No	No	No	No	No	No	No	No	Yes	Yes	Yes	Yes	
No	No	No	No	No	No	No	No	No	No	No	No	Yes	Yes	Yes	
No	No	No	No	No	No	No	No	No	No	Yes	Yes	Yes	Yes	Yes	
No	No	No	No	No	No	No	Yes	Yes	Yes	Yes	Yes	Yes	Yes	Yes	C(2)
No	No	No	No	No	No	No	No	Yes	Yes	Yes	Yes	Yes	Yes	Yes	
No	No	No	No	No	No	No	No	No	No	No	No	Yes	Yes	Yes	D(1)

Figure 4-b. Detected programmed defects based on optical inspection on wafer with metal oxide stack

15	14	13	12	11	10	9	8	7	6	5	4	3	2	1	PD
NA	NA	NA	NA	NA	NA	0	0	0	11	26	18	11	42	16	A(4)
NA	0	0	0	0	0	0	0	0	0	13	8	45	13	47	B(3)
NA	0	0	0	0	0	0	0	0	0	0	21	21	24	37	
NA	NA	NA	0	0	0	0	0	0	0	0	0	18	39	45	
NA	0	0	0	0	0	0	0	0	0	5	26	21	39	29	
0	0	0	0	0	0	0	29	42	97	92	97	100	100	97	C(2)
0	0	0	0	0	0	0	0	32	74	95	89	100	100	100	
0	0	0	0	0	0	0	0	0	0	0	0	26	63	82	D(1)

Figure 4-c. PD capture rate in percentage normalized by printability on wafer with metal oxide stack

Figure 5 shows the results of optical inspection for the wafer with CAR stack. Optical sensitivity on CAR stack is significantly better and no further improvement was necessary. For the metal oxide case, we investigated methods to improve signal-to-noise ratio for programmed defects for optimized defect capture.

Decreasing Size ←

15	14	13	12	11	10	9	8	7	6	5	4	3	2	1	PD
No	No	No	No	No	No	Yes	Yes	Yes	Yes	Yes	Yes	Yes	Yes	Yes	A(4)
No	No	No	No	No	No	Yes	Yes	Yes	Yes	Yes	Yes	Yes	Yes	Yes	B(3)
No	No	No	No	No	No	Yes	Yes	Yes	Yes	Yes	Yes	Yes	Yes	Yes	
No	No	No	No	No	No	Yes	Yes	Yes	Yes	Yes	Yes	Yes	Yes	Yes	
No	No	No	No	No	No	Yes	Yes	Yes	Yes	Yes	Yes	Yes	Yes	Yes	
No	No	No	Yes	Yes	Yes	Yes	Yes	Yes	Yes	Yes	Yes	Yes	Yes	Yes	C(2)
No	No	No	Yes	Yes	Yes	Yes	Yes	Yes	Yes	Yes	Yes	Yes	Yes	Yes	
No	No	No	No	No	Yes	Yes	Yes	Yes	Yes	Yes	Yes	Yes	Yes	Yes	D(1)

Figure 5. Detected programmed defects based on 3905 optical inspection on wafer with CAR stack

3.3 Electromagnetic Simulations and Optical Wafer Inspection

One of the ways to identify possible improvements in signal-to-noise ratio and hence defect capture is to perform rigorous electromagnetic (EM) simulations. Typically, in such situations, EM studies are done to discover the optimal optical setting of the inspection tool. However, it can also be used to suggest alternative underlying materials or stack, especially in cases where sensitivity is limited by stack properties such as refractive index (n), dielectric constant (k) or film thickness. This approach is called *stack engineering*. Although it may not be applicable for a production process scenario, where changing the stack is not desirable or may even be impossible, for monitoring or qualification purposes in high volume manufacturing, it is certainly possible to have an alternative stack on a short loop wafer, especially if the underlying process is relatively inexpensive.

Figure 6 shows output from such an exercise, using an oxide underlayer instead of SoC. The result shows significant improvement.

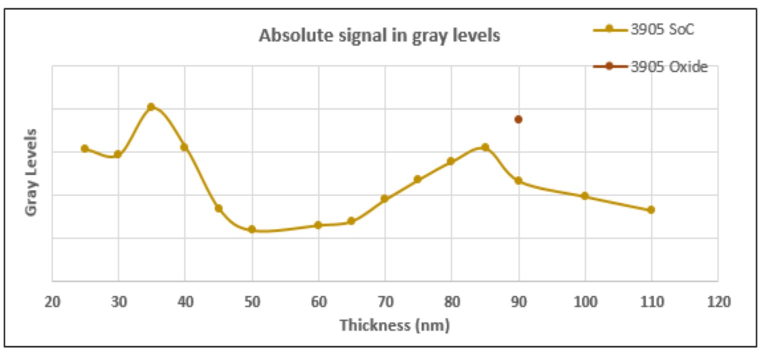

Figure 6. Simulated signals with oxide underlayer as compared to POR SoC.

Short-loop wafers were prepared with 90 nm oxide underlayer and optical inspections were performed using the 3905 optical inspection tool to validate the improvement. Since the stack has changed, we needed to revisit the printability of programmed defects to establish the ground truth and optimize the optical settings of the inspection tool. Figure 7a shows the result of the printability study using eDR7280 Critical Point Imaging (CPI) mode. Figure 7b shows the average optical signal-to-noise ratio for one of the large PD of type B. SNR improves on an average by a factor of 3.5. Consequently, the capture rate of programmed defects increases by a factor of 9x, as shown in figure 7c.

Decreasing Size ←

15	14	13	12	11	10	9	8	7	6	5	4	3	2	1	PD
0	0	0	0	0	0	100	89	100	100	100	100	100	100	100	A(4)
0	0	0	0	11	0	78	100	100	100	100	100	100	100	100	B(3)
0	0	0	0	0	0	67	89	100	100	100	100	100	100	100	
0	0	0	0	0	44	67	100	100	100	100	100	100	100	100	
0	0	0	0	0	56	78	100	100	100	100	100	100	100	100	
0	44	56	56	67	100	100	100	100	100	100	100	100	100	100	C(2)
0	0	33	67	89	100	100	100	100	100	100	100	100	100	100	
22	44	78	89	100	100	100	100	100	100	100	100	100	100	100	D(1)

PD Type

Figure 7-a. Percentage of locations where a defect was visible on SEM across multiple fields on a wafer with oxide underlayer & metal oxide resist

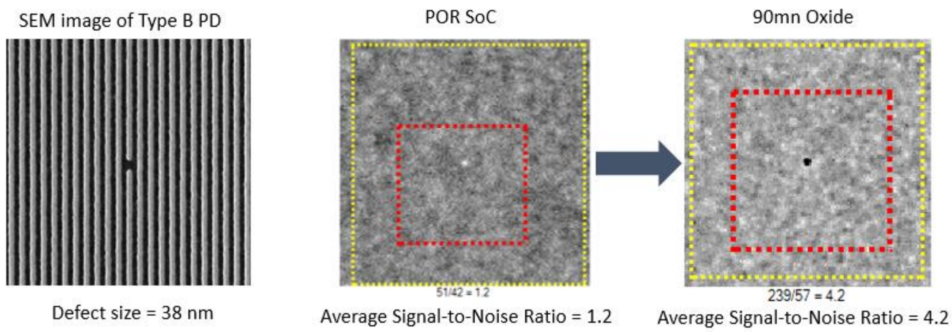

Figure 7-b. 3905 signal-to-noise ratio improvement by changing underlayer to oxide from SoC for the metal-oxide resist wafer

15	14	13	12	11	10	9	8	7	6	5	4	3	2	1	PD
NA	NA	NA	NA	NA	NA	0	0	91	98	100	100	100	100	100	A(4)
NA	NA	NA	NA	0	NA	0	0	0	0	100	100	100	100	100	B(3)
NA	NA	NA	NA	NA	NA	0	0	2	2	9	100	100	100	100	
NA	NA	NA	NA	NA	0	0	0	0	34	100	100	100	100	100	
NA	NA	NA	NA	NA	0	0	0	4	13	98	100	100	100	100	
NA	0	0	0	0	2	17	96	100	100	100	100	100	100	100	C(2)
NA	NA	0	0	0	2	21	15	100	100	100	100	100	100	100	
0	0	0	0	0	2	0	4	21	60	62	79	100	100	100	D(1)

Figure 7-c. Percentage PD capture rate using 3905 optical inspection tool normalized by printability for oxide underlayer wafers with metal-oxide resist

Hence, as demonstrated, stack engineering is a very useful approach to enhance sensitivity and capture rate for defects of interest. Once adequate sensitivity is obtained, the main purpose of optical inspection is to study and track the capture of natural repeaters, mask defects that have not been intentionally programmed. These defects may accumulate on the mask over time from various sources, for example, mono-layer deposition from the vacuum system and growth of haze defects or other film or particle depositions on the reticle. With a reliable wafer level defect inspection in place, the locations of these mask defects can be identified. Figure 8 shows the improvement in natural repeaters identified on the metal oxide resist with stack engineering. Having optimal sensitivity at the wafer level is very important for identifying both hard repeaters and soft repeaters. Although we have not done specific sizing of the defects, it is evident that majority of the improvement comes from capture of smaller defects, which were missed earlier due to weak signal to noise ratio. These locations can now be monitored with time. Any increase beyond statistical variation indicates added contamination on the mask and hence appropriate control action is required.

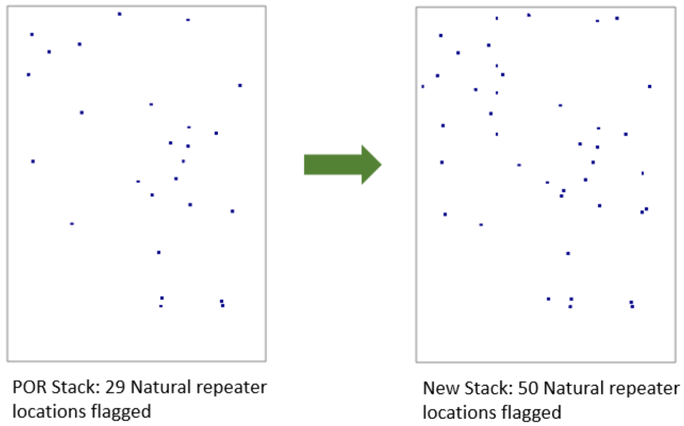

Figure 8. 72% improvement in natural repeaters with stack engineering

4. CONCLUSIONS

As EUV moves towards high volume manufacturing there is a need to provide not only mask qualification but also re-qualification techniques. In this paper, we described a method for in-fab EUV mask qualification and re-qualification to identify additional contamination over time. Optical wafer inspection techniques using KLA-Tencor's 3905 broadband plasma inspection system proved to be a valuable alternative to mask inspection, especially when dealing with pellicle uncertainty. Also, defect printability variation can be quantified through confirmation on the wafer. Because these variations can cause soft repeaters, high sampling across the wafer is required, which is with the hallmark of optical inspection methods. We compared two resist types that were challenging for optical inspection based on material properties, thickness and underlying stack. Through simulations we have shown that it is possible to overcome these challenges, and we conclude that stack engineering can result in significant improvement of repeater capture. In our future study we will monitor natural repeaters periodically to enable timely identification of mask contamination excursions.

REFERENCES

[1] Britt Turkot (Intel Corp.) keynote presentation, "EUVL Readiness for High-Volume Manufacturing" 2017 SPIE Advanced Lithography conference